ACS APPLIED MATERIALS & INTERFACES

Research Article

www.acsami.org

Interface Chemistry and Molecular Bonding of Functional Ethoxysilane-Based Self-Assembled Monolayers on Magnesium Surfaces

Manuela S. Killian,[†] Steffen Seiler,[‡] Victoria Wagener,[†] Robert Hahn,[†] Christina Ebensperger,[‡] Bernd Meyer,[‡] and Patrik Schmuki*[,†,¶]

[†]Department of Materials Science and Engineering, Chair for Surface Science and Corrosion, Friedrich-Alexander-University Erlangen-Nürnberg, Martensstrasse 7, 91058 Erlangen, Germany

[‡]Interdisciplinary Center for Molecular Materials (ICMM) and Computer-Chemistry-Center (CCC), Friedrich-Alexander-University Erlangen-Nürnberg, Nägelsbachstrasse 25, 91052 Erlangen, Germany

[¶]Department of Chemistry, King Abdulaziz University, Jeddah 22254, Saudi Arabia

Supporting Information

ABSTRACT: The modification of magnesium implants with functional organic molecules is important for increasing the biological acceptance and for reducing the corrosion rate of the implant. In this work, we evaluated by a combined experimental and theoretical approach the adsorption strength and geometry of a functional self-assembled monolayer (SAM) of hydrolyzed (3-aminopropyl)-triethoxysilane (APTES) molecules on a model magnesium implant surface. In time-of-flight secondary ion mass spectrometry (ToF-SIMS) and X-ray photoelectron spectroscopy (XPS), only a minor amount of reverse attachment was observed. Substrate−O−Si signals could be detected, as well as other characteristic APTES fragments. The stability of the SAM upon heating in UHV was investigated additionally. Density-functional theory (DFT) calculations were used to explore the preferred binding mode and the most favorable binding configuration of the hydrolyzed APTES molecules on the hydroxylated magnesium substrate. Attachment of the molecules via hydrogen bonding or covalent bond formation via single or multiple condensation reactions were considered. The impact of the experimental conditions and the water concentration in the solvent on the thermodynamic stability of possible APTES binding modes is analyzed as a function of the water chemical potential of the environment. Finally, the influence of van der Waals contributions to the adsorption energy will be discussed.

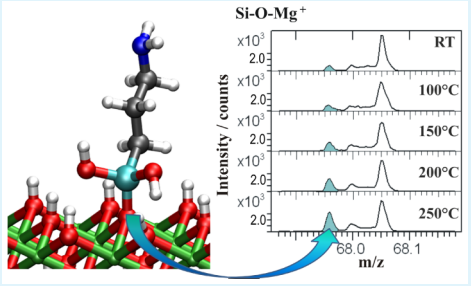

KEYWORDS: *magnesium, self-assembled monolayer, silane coupling, ToF-SIMS, DFT calculations*

INTRODUCTION

Amine-terminated alkoxysilane thin films find extensive application in a wide variety of both industrial and research-oriented applications, ranging from adhesion promotion of polymer films on glass,[1,2] fiberglass−epoxy composites,[3−6] and attachment of (noble) metal nanoparticles to silica substrates,[7,8] to biomedical applications. For the latter, specifically (3-aminopropyl)triethoxysilane (APTES) is used in lab-on-a-chip applications[9−11] or as bioactive linker to promote protein adhesion to oxide surfaces relevant in implant technology, for example, titanium (with a TiO_2 surface)[12−15] or magnesium (with OH-termination under physiological conditions).[16,17]

Whereas titanium is mainly used as implant because of its inertness, strength and lightness, magnesium can find application in biodegradable implant devices, for example, as nonpermanent orthopedic implant or stent in cardiovascular surgery.[18,19] It dissolves in aqueous environments and the dissolved magnesium ions produced in the degradation are believed to be rather beneficial for the human organism.[20] Unfortunately, corrosion of pure magnesium occurs very fast under physiological conditions[21] and the accompanying hydrogen evolution is of concern.[21−23] It has been reported that albumin coatings of magnesium can lower the corrosion rate of magnesium in simulated body fluid,[24,25] and it can be decreased to a greater extent if APTES and ascorbic acid are used as linker units.[16,17] A SAM of APTES alone was shown to significantly slow down the corrosion of a magnesium surface.[16]

Under atmospheric conditions and in aqueous environments $Mg(OH)_2$ forms at the Mg surface. To the current state of knowledge, however, it is not completely understood whether the APTES linker is covalently attached to the hydroxylated Mg substrate or just weakly bonded and in which orientation the bifunctional molecule is adsorbed on the surface. A covalent bond formation to silicon or titanium dioxide substrates is

Received: October 31, 2014
Accepted: March 18, 2015
Published: March 18, 2015

DOI: 10.1021/am5075634
ACS Appl. Mater. Interfaces 2015, 7, 9006−9014

assumed for ethoxy-, methoxy- and chlorosilanes.[26−33] The available literature suggests that time-of-flight secondary ion mass spectrometry (ToF-SIMS) and X-ray photoelectron spectroscopy (XPS) are valuable tools for elucidation of the adsorption mechanism and orientation of the SAM. XPS as well as infrared spectroscopy can determine, for example, the state of the amino group of the adsorbed APTES molecule,[34,35] whereas ToF-SIMS has the capability to provide information on the binding strength of a SAM to the substrate. Nie[36] investigated the adsorption of phosphonic acids to silicon and aluminum oxides with ToF-SIMS and concluded that the occurrence of dimers is indicative of weakly bonded species, whereas strong, covalent bonds lead to "substrate + molecule" fragments. Killian et al. investigated the binding mechanism of a zinc porphyrin containing an APTES functional group (Zn(II)-5-(tris-ethoxy-silane-propyl-amide-acetato-phenoxy)−10,15,20-(p-*tert*-butyl-triphenyl)-porphyrin, Zn-TESP) to silicon and titanium oxide as well as to hydroxylated magnesium.[37,38] For the physisorbed molecule the molecular fragment M^+ was observed and for stronger bonded forms of the immobilized Zn-TESP cleavage between the Si headgroup and the organic rest of the molecule (Si-R) occurred upon fragmentation. A strong interaction of the molecule also to hydroxylated Mg substrates was determined. Cleavage of the Si-R bond was also observed for UV irradiation of the APTES modified porphyrin Zn-TESP immobilized on TiO_2[39] and for ion bombardment of APTES SAMs in ToF-SIMS.[32] Castner et al. focused on the binding of (3-methacryloxypropyl) trimethoxysilane to TiO_2 in a multitechnique approach via ToF-SIMS, XPS, and AFM, where covalent attachment of the methoxysilane to TiO_2 was also concluded.[40]

Density-functional theory (DFT) calculations can provide direct atomistic insights into surface and adsorbate structure and the nature of molecule−substrate interactions. DFT calculation have been used, for example, to elucidate the preferred binding mode of long alkyl chains with phosphonic and carboxylic acid head groups on hydroxylated Al_2O_3 substrates.[41] Furthermore, the stability of the possible binding modes depending on experimental conditions has been analyzed by combining DFT results with a thermodynamic analysis.[41] Compared to Al_2O_3, the surface chemistry of magnesium hydroxide is much less explored. We are aware of only two DFT studies on the reaction with HF and the degradation of sarin.[42,43]

METHOD SECTION

All chemicals were purchased by chemical suppliers and used without further purification. All organic solvents were of water-free grade.

Substrate Preparation. Samples were cut off a pure magnesium rod (ChemPur Feinchemikalien und Forschungsbedarf GmbH, 99.9% purity, 25.4 mm diameter) as discs with average height of 2−3 mm. All samples were polished to a 0.2 μm finish with abrasive cloth using diamond- and fumed-silica suspension for a total of 15 min, the last 15 s H_2O was used as rinsing agent. The samples were kept under atmospheric conditions until further investigation or functionalization. The surface composition was examined by XPS and as a ratio of Mg/O of 1:2 was observed, we conclude that the material consists of $Mg(OH)_2$ within the information depth of XPS (~10 nm). SEM showed that the surface was smooth after polishing and no incorporation of silica particles was observed.

SAM Formation. Silanization of the surface with (3-aminopropyl) triethoxysilane (APTES) was achieved by refluxing of the substrates in a 10 mM APTES solution in water-free grade toluene (Aldrich, 99.8% purity) to prevent any polymerization for 24 h at 70 °C.[14,45] The samples were thoroughly rinsed with acetone and ethanol, followed by ethanol ultrasonic treatment. According to Brzoska et al.[44] the APTES molecule is hydrolyzed to (3-aminopropyl)trihydroxysilane (APTHS) in contact with the adsorbed water layer on the oxide surface.

Surface Analysis. Positive and negative static SIMS measurements were performed on a ToF.SIMS-5 spectrometer (ION-TOF, Münster). The samples were irradiated with a pulsed 25 keV Bi_3^+ ion beam. Spectra were recorded in the high mass resolution mode ($m/\Delta m$ > 8000 at ^{29}Si). The beam was electrodynamically bunched down to <1 ns to increase the mass resolution and scanned over a 500 × 500 μm^2 area. The primary ion dose density (PIDD) was kept at 1 × 10^{11} ions/cm^2, ensuring static conditions. Signals were identified using the accurate mass, as well as their isotopic pattern. Poisson correction was used for integration of the signal intensities. Spectra were normalized to their total intensity and calibrated on CH_3^+, $C_2H_3^+$, $C_3H_5^+$, $C_4H_9^+$, and $C_7H_7^+$ signals for positive and CH_2^-, C_2^-, CN^-, and CNO^- for negative spectra.

For desorption experiments the samples were heated with a rate of 1 K/s in vacuum ($\lesssim 5 \times 10^{-8}$ mbar) up to a temperature of 250 °C. Measurements were taken every 50 °C after the temperature was kept constant for 30 min each. This procedure is reported to be sufficient to remove physisorbed species.[46] As the experiment requires the sample not to be moved, 10 subsequent measurements with a PIDD of 1 × 10^{11} ions/cm^2 each were conducted on the same area.

X-ray photoelectron spectra (XPS) were recorded on a PerkinElmer Physical Electronics 5600 spectrometer using monochromated Al Kα radiation (1486.6 eV; 300 W) as excitation source. The takeoff angle of the emitted photoelectrons was 45° (the angle between the plane of sample surface and the entrance lens of the detector). The binding energy of the target elements (O 1s, C 1s, N 1s, Mg 2p, Si 2p) was determined at pass energy of 23.5 eV, values were recorded every 0.2 eV and the binding energy of the C 1s signal (284.8 eV) was used as reference. The measurement spot had a diameter of 800 μm and 100 cycles were recorded for each spectrum. The background was subtracted using the Shirley method in all spectra. To obtain the molar fractions of each species, the peak areas of the measured XPS spectra were corrected with the photoionization cross sections of Scofield[47] σ and the asymmetry parameter β (orbital geometry),[48] which are contained in the sensitivity factors of the acquisition software (MultiPak V6.1A, 99 June 16, Copyright Physical Electronics, Inc., 1994−1999).

DFT. Periodic slab calculations were performed with the plane-wave code `PWscf` of the Quantum Espresso software package[49] using Vanderbilt ultrasoft pseudopotentials[50] and the PBE exchange-correlation functional.[51] A kinetic energy cutoff for the plane-wave basis of 25 Ry and a (2 × 2 × 1) Monkhorst−Pack k-point grid for $Mg(OH)_2$ slabs with a (3 × 3) surface unit cell size is sufficient to get well-converged results for structures and adsorption energies. Geometries were optimized by minimizing the atomic forces, with a convergence threshold for the largest residual force component of 5 meV/Å.

The influence of dispersion effects was tested by adding semiempirical pairwise C_6/R^6 van der Waals correction terms (multiplied by a damping function at short distances and a functional-dependent scaling factor) to the DFT energy functional. The C_6 coefficients and the damping functions were chosen according to the Grimme D2 scheme,[52] except for Mg. Here, a modified C_6 value was used, which was adjusted to be more appropriate for ionic crystals.[53−55] In the following we will refer to this setup as PBE+D2*. Despite the modification of the C_6 parameter for Mg, benchmark tests for water adsorption on MgO and $Mg(OH)_2$ model clusters still showed an overbinding for such configurations dominated by hydrogen bonds.[55] Therefore, the PBE+D2* adsorption energies reported here should only be taken as lower bounds for the influence of dispersion interactions. Fortunately, it turned out that the D2* correction only leads to an overall lowering of the adsorption energies but does not change the qualitative picture concerning the preferred binding modes and the relative thermodynamic stability of different structures.

The OH-terminated Mg surfaces were modeled by periodic slabs built from the brucite $Mg(OH)_2$ structure with (0001) surface

DOI: 10.1021/am5075634
ACS Appl. Mater. Interfaces 2015, 7, 9006−9014

terminations. The structure consists of well-ordered hexagonal HO−Mg−OH triple layers with an fcc stacking sequence. All calculations were done for slabs with a (3 × 3) surface unit cell and a thickness of two $Mg(OH)_2$ triple layers, resulting in a total number of 90 substrate atoms in the unit cell. A vacuum region of about 10 Å prevented electronic interactions between adjacent periodic replica in the direction perpendicular to the surfaces. In the geometry optimization, only the atoms in the upper $Mg(OH)_2$ triple layer were allowed to relax, whereas the atoms in the bottom triple layer were kept fixed at the lattice positions of the brucite crystal as determined from a previous DFT bulk calculation. With our DFT-PBE setup we obtained bulk lattice constants of a = 3.194 Å and c = 4.844 Å (c/a = 1.517), which deviate only by 1.4% and 1.6% from the respective experimental values of a = 3.150 Å and c = 4.770 Å (c/a = 1.514).[56]

In the experiments it can be assumed that most of the APTES molecules instantaneously hydrolyze to (3-aminopropyl)-trihydroxysilane (APTHS) when they come in contact with residual water on the hydroxide surface.[44] We therefore started our theoretical investigations of the adsorption process immediately from the APTHS molecule with a silanol headgroup. APTHS adsorption energies were calculated according to

$$E_{ad} = [(E_{slab}^{ad} + n\,E_{mol}^{W}) - (E_{slab}^{bare} + N\,E_{mol}^{APTHS})]/N \quad (1)$$

where N is the number of adsorbed APTHS molecules on the $Mg(OH)_2$ slab and n is the number of removed water molecules after condensation reactions of APTHS with the surface. E_{slab}^{ad} and E_{slab}^{bare} are the total energies of two slab calculations with and without adsorbates, and E_{mol}^{W} and E_{mol}^{APTHS} are the total energies of a gas phase water and APTHS molecule, respectively. These reference energies were determined by placing the isolated molecules into a large vacuum box.

RESULTS AND DISCUSSION

The self-assembly of APTES on polished hydroxylated Mg discs was conducted in water-free solvent. No visible corrosion of the surface occurs during this treatment, the Mg disc still shows a mirror-finish after functionalization. The chemical formula of the APTES molecule is shown in Figure 1a. Figure 1b displays the atomic composition determined by XPS for an untreated surface and an APTES SAM on the hydroxylated Mg. The ratio of Mg:O indicates the presence of at least 10 nm of $Mg(OH)_2$ for the pristine disc. Compared to a polished Mg reference, the APTES coated substrate discs display clear N 1*s* and Si 2*p* signals in XPS (with atomic concentrations of 5.7% each), whereas the Mg signal strongly decreases upon functionalization. The excess carbon can be explained by toluene coadsorption, residual contamination (the excess at% of C 1*s* with respect to a 1:3 C:Si or C:N stoichiometry is approximately equivalent to the initial carbon content on the pristine Mg surface) or unreacted ethoxy side chains. The latter can occur if APTES preferentially attaches to the substrate via a single ethoxy functionality. As the reaction is conducted in water-free environment (apart from some residual water on the hydroxylated Mg surface[44]), ethoxy groups that do not undergo condensation reactions with the substrate may retain unreacted. The peak position of the O 1*s* signal of the APTES SAM lies at a lower binding energy than the O 1*s* signal of the thick APTES layer (but higher than the oxide, see Supporting Information Figure S1). This indicates a transformation of Si−O−C_2H_5 to Si−O−Mg or Si−O−Si, the binding energy of the oxygen atom is expected to decrease in this case.

Horner et al.[34] adsorbed APTES out of an aqueous solution to various metal surfaces and correlated the state of the amino group determined by angle resolved XPS with the orientation of the molecule and also the isoelectric point (IEP) of the substrate. NH_3^+ signals were observed to originate from the

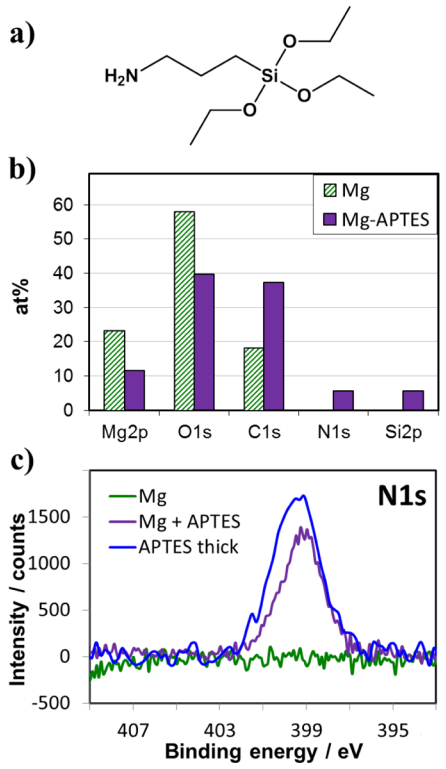

Figure 1. (a) Chemical formula of the APTES molecule. (b) Atomic percentages of the elements detected by XPS on the pristine and APTES functionalized OH-terminated Mg surface. (c) N 1*s* signal of bare Mg, APTES coated Mg, and a thick layer of APTES.

substrate−APTES rather than from the APTES−air interface, indicating a reverse adsorption of the molecule. Additionally, Song et al. determined the orientation of the APTES molecule on titanium substrates of different crystallinity by examination of the N 1*s* signal.[45] For reverse attachment of APTES, the protonated $-NH_3^+$ group can coordinate to surface hydroxyl groups, a higher N 1*s* binding energy of 400.9 eV was observed. Coordination via the ethoxysilane groups yields a $-NH_2$ terminated surface with an amine signal at 399.4 eV. Thus, from the position of the N 1*s* signal at 399.1 eV in Figure 1c it can be concluded that the amine group mainly exists as $-NH_2$, excluding reverse attachment of APTES on hydroxylated Mg substrates. The slight deviation of the two results can be explained by the fact that the measurements recorded by Song et al.[45] were corrected for the Ti 2*p* binding energy, whereas the data presented in this manuscript was shifted to the C 1*s* binding energy. The N 1*s* signal of a thick APTES layer produced by evaporation of a droplet of APTES solution (multilayer sample) is significantly broadened and shifted to higher binding energies, indicating random orientation and a possible coordination of the APTES amino groups to the ethoxysilane moieties. The affinity for covalent attachment of APTES (the pH of 10 mM APTES in an aqueous environment is 11.2) is in agreement with the different isoelectric points (IEP) of the substrates. The surface of $Mg(OH)_2$ (IEP = 11.6−13.2)[57] will be rather positively charged and TiO_2 (IEP = 5.1−6.4)[57] will have a negative surface charge and consequently be able to bind APTES via ionic interaction with the protonated amino group.

As the N 1*s* binding energy in XPS is an indication for but not a direct proof of covalent bonding, the adsorbed linker

DOI: 10.1021/am5075634
ACS Appl. Mater. Interfaces 2015, 7, 9006−9014

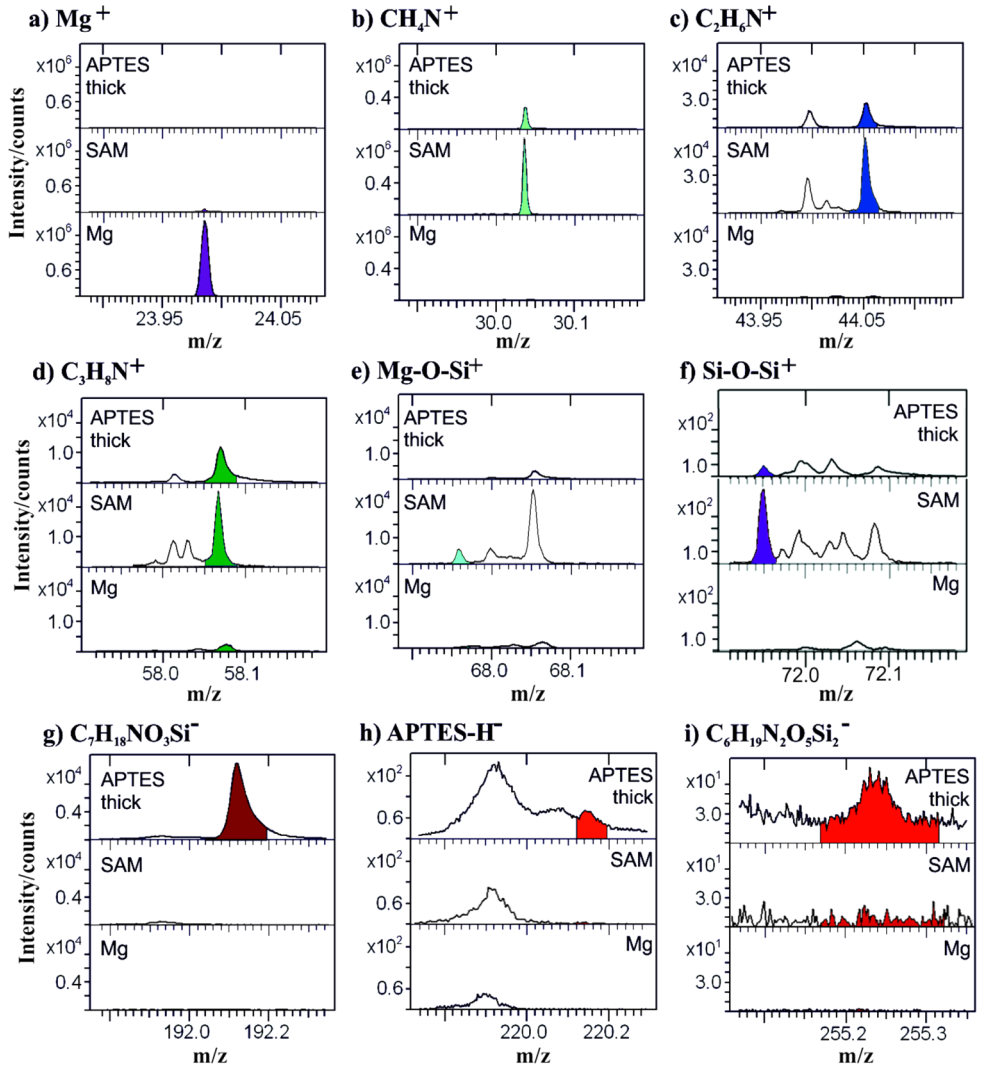

Figure 2. Relevant ToF-SIMS signals (colored) of a thick layer of APTES on a OH-terminated Mg substrate (top), a SAM of APTES on hydroxylated Mg (middle) and APTES-free Mg (bottom): (a) signal of the substrate, m/z = 23.99 − Mg^+; (b–d) fragments characteristic for chemisorbed APTES (b) m/z = 30.03 − CH_4N^+, (c) m/z = 44.05 − $C_2H_6N^+$, (d) m/z = 58.07 − $C_3H_8N^+$; (e) APTES bound to the substrate, m/z = 67.96 − Si−O−Mg^+; (f) cross-linking of APTES, m/z = 71.95 − Si−O−Si^+; (g–i) fragments characteristic of physisorbed APTES (g) APTES hydrolyzed in one single ethoxysilane group, m/z = 192.12 − $C_7H_{18}NO_3Si^-$, (h) molecular fragment M−H^-, m/z = 220.15 − $C_9H_{22}NO_3Si^-$, (i) dimer of the hydrolyzed form of APTES, m/z = 255.23 − $C_6H_{19}N_2O_5Si_2^-$.

molecule was additionally investigated with ToF-SIMS, as this technique can show bond formation, for example, by the occurrence of substrate–molecule fragments. For more detailed investigation of the adsorbed linker molecule, an APTES self-assembled monolayer was examined by ToF-SIMS alongside two references: a thick APTES coating (multilayer sample) and a pristine Mg disc. Figure 2 shows selected characteristic fragments in detailed resolution: the top panel in each subfigure displays the fragments caused by the thick APTES coating, the middle panel contains the spectrum of the APTES SAM and the bottom panel presents pristine OH-terminated Mg. The assignment of all signals visible in the displayed spectral regions can be found in the Supporting Information, Table S1.

In the positive polarity spectra of Figures 2a–d, the decrease of Mg^+ accompanied by an increase in characteristic APTES fragments CH_4N^+, $C_2H_6N^+$, and $C_3H_8N^+$ suggests the presence of APTES on the substrate. On the multilayer sample no Mg^+ could be detected, indicating that the coating thickness exceeded the ToF-SIMS information depth (~1–3 nm). The signals characteristic of APTES (Figures 2b–d) are significantly enhanced on the monolayer sample compared to the multilayer sample. This effect has been reported previously for ethoxysilanes covalently attached to the substrate,[16,37] as the Si–C bond can be weakened upon the formation of an Si–O–substrate bond, causing preferred ionization of the residual part of the molecule (i.e., CH_4N^+, $C_2H_6N^+$, or $C_3H_8N^+$). The formation of Si–O–substrate bonds for the APTES SAM is indicated by the presence of the fragment Mg–O–Si^+ (see Figure 2e), which can only be produced if the condensation reaction with the substrate was successful. Furthermore, the intensity of Si–O–Si fragments is clearly increased on the SAM sample, indicating the cross-linking of free ethoxysilane groups and siloxane formation (see Figure 2f). The average relative intensities of these signals with respect to the total intensity of the spectrum are increasing from 0.00091% (thick) to 0.031% (SAM) for Mg–O–Si^+ and from 0.011% (thick) to 0.069% (SAM) for Si–O–Si^+.

DOI: 10.1021/am5075634
ACS Appl. Mater. Interfaces 2015, 7, 9006–9014

The negative polarity spectra of the thick layer of APTES show several fragments indicative of weakly bound APTES (Figures 2g–i). The molecule hydrolyzed in one single ethoxysilane group, as well as the intact molecular fragment, could be clearly identified. The latter can only be caused by physisorbed molecules that did not complete a condensation reaction with the substrate (i.e., loose ethanol in this process). Furthermore, a clear signal of the dimer of the hydrolyzed form of APTES was detected in the thick layer sample. According to Nie et al.,[36] dimeric fragments are characteristic for weakly bound, physisorbed molecules. These signals could only be detected on the multilayer reference sample, but not on the SAM coated Mg surface.

The combined information obtained by ToF-SIMS and XPS consistently suggest a strong bond formation of the APTES molecules with the OH-terminated Mg substrate, with a major fraction of the molecule coordinating via the ethoxysilane functional group.

To investigate the stability of the SAM on hydroxylated Mg, that is, the interaction strength of the linker molecules with the substrate, an APTES coated Mg disc was heated to 250 °C in UHV. This procedure was reported to be sufficient to remove physisorbed species.[46] The sample was heated in the ToF-SIMS instrument and measurements were recorded every 50 °C. The Mg^+, $Mg–O–Si^+$, and $Si–O–Si^+$ signals were observed to increase slightly, whereas the fragments characteristic of APTES stay approximately constant (see Figure 3). The increase in Mg^+ can mainly be related to desorbing contaminations (hydrocarbons, phthalate, see Figure S2 in the Supporting Information), uncovering the substrate. The increase of $Mg–O–Si^+$ may be caused by the aforementioned reason, condensation reactions between free ethoxysilane groups of APTES molecules and the substrate, or by a greater extent of fragmentation of the molecules caused by repeated ion bombardment of the sample (a maximal primary ion dose of 1×10^{12} ions/cm^2, well below the static limit, was applied). The $Si–O–Si^+$ signal also increases with sample temperature, which can be caused by the aforementioned reasons or increased cross-linking with additional activation energy, indicating that the adsorbed APTES molecules possess free silanol groups. The remaining presence of the APTES fragments shows that a major part of the SAM is not removable by heat, and again suggests a strong bond formation.

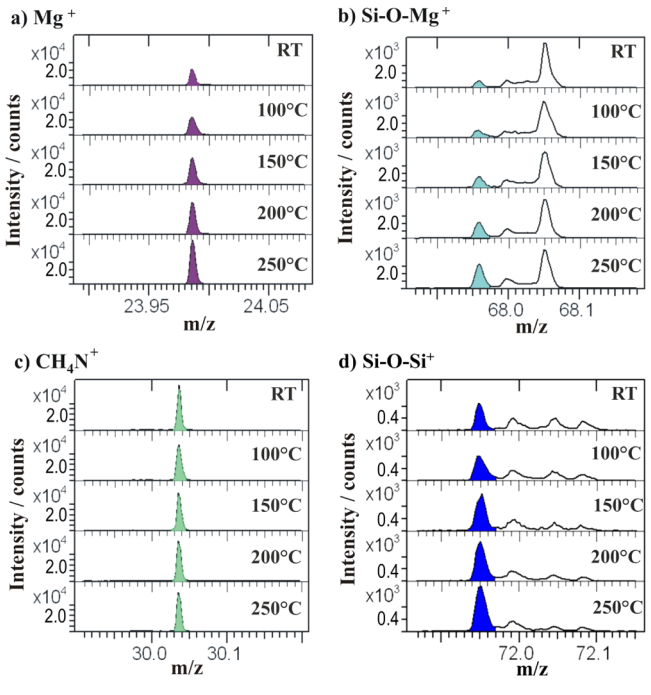

Figure 3. SAM of APTES on OH-terminated Mg was heated in UHV to 250 °C to investigate desorption and interaction strength. The signal of the Mg substrate, m/z = 23.99 – Mg^+, is displayed in panel (a). Panel (b) shows the APTES bond to the substrate m/z = 67.96 – $Si–O–Mg^+$, while (c) displays a fragment characteristic for APTES, m/z = 30.03 – CH_4N^+. (d) shows the $Si–O–Si^+$ bond (m/z = 71.95), indicative of cross-linked APTES. The discussed signals are colored in the spectra.

In addition, DFT calculations were performed to analyze in detail the interaction of hydrolyzed APTES molecules (APTHS) with a $Mg(OH)_2$ substrate. First, different binding modes via the silanol group of the APTHS molecules were probed. Attachment of the $Si(OH)_3$ group to the surface by noncovalent interactions via H-bonds (physisorption) or by forming covalent bonds via one, two and three condensation reactions (chemisorption), giving rise to mono-, bi- and tridentate surface species, respectively, were considered. Each condensation reaction releases one water molecule into the environment:

$$Mg(OH)_2 + Si(OH)_3C_3H_6NH_2 \rightarrow (HO)Mg\text{-}O\text{-}Si(OH)_2C_3H_6NH_2 + H_2O \quad (2)$$

In both physisorption and chemisorption different H-bonding patterns can be present, depending on whether the OH-groups of the $Si(OH)_3$ silanol functional group donate or receive an H-bond from the surface (see Figure 4). Therefore, geometry optimizations were performed for a set of initial geometries which differ in the orientation of OH-groups and the relative position of the molecule above the surface.

The results for the most stable APTHS configurations for each binding mode are shown in Figure 4 and the corresponding adsorption energies are summarized in Table 1. Noncovalent binding gives the lowest adsorption energy. In the most favorable structure, all three OH-groups of the APTHS molecule donate an H-bond to surface OH. The surface OH-groups are tilted out of their normal orientation in order to be able to receive the H-bond (see Figure 4a). Monodentate covalent binding via one condensation reaction, however, is only slightly less favorable (see Table 1). Bi- and tridentate binding, on the other hand, give positive adsorption energies, indicating that the second and third subsequent condensation reaction between substrate and the APTHS linker are endothermic. The reason is mostly geometric: the hydroxyl groups on the surface are too far apart so that the $Si(OH)_3$ group has to distort in order to be able to form two or three covalent bonds to the surface. The results in Table 1 show that the adsorption energies decrease significantly when the semiempirical D2* dispersion correction is used. However, the order of relative stability of the four binding modes remains unchanged.

In a second set of DFT calculations, alternative binding modes for the hydrolyzed APTES molecules were considered. Figure 5a and b show two possible configurations for noncovalent attachment of the linker molecules via their amino group. The adsorption energies in Table 1 indicate, however, that these molecule–substrate interactions are rather weak and much less favorable than physisorption and

DOI: 10.1021/am5075634
ACS Appl. Mater. Interfaces 2015, 7, 9006–9014

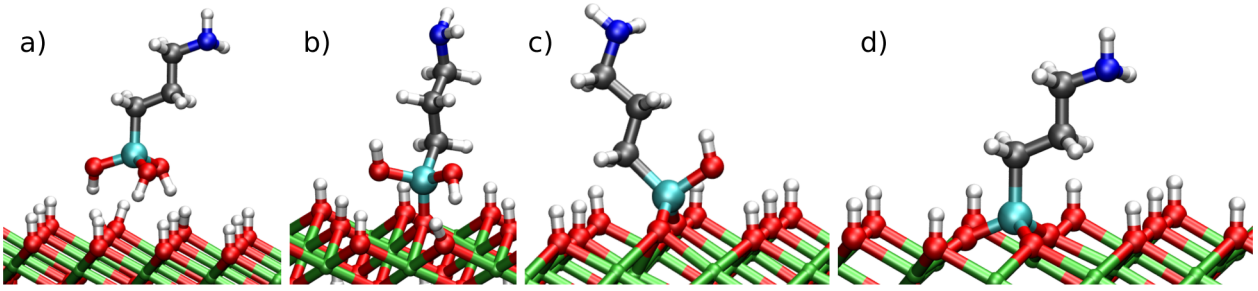

Figure 4. Most stable configuration of hydrolyzed APTES on $Mg(OH)_2$ for different binding modes via the silanol group: (a) noncovalent bonding (physisorption), (b) mono-, (c) bi-, and (d) tridentate covalent bonding after one, two, and three condensation reactions have occurred, respectively. Magnesium atoms are shown in green, oxygen in red, hydrogen in white, carbon in black, silicon in cyan, and nitrogen in blue.

Table 1. PBE and PBE+D2* Adsorption Energies E_{ad} (in eV) per Hydrolyzed APTES Molecule (APTHS) on $Mg(OH)_2$ for Different Binding Configurations

		PBE	PBE+D2*
physisorbed	Figure 4a	−0.38	−0.91
monodentate	Figure 4b	−0.27	−0.74
bidentate	Figure 4c	+0.77	+0.49
tridentate	Figure 4d	+1.53	+1.40
amine, donating	Figure 5a	−0.10	−0.36
amine, accepting	Figure 5b	−0.12	−0.29
APTHS, flat	Figure 5c	−0.27	−0.91
cross-coupled	Figure 5d	−0.11	−0.60

chemisorption via the silanol group. Thus, reverse attachment of the APTHS molecules to the hydroxylated Mg substrate will not play an important role, as already discussed in the experimental section.

Calculations were not only performed for upright-standing linker units, but also for molecules lying flat on the surface. Figure 5c shows the most stable structure of a monodentate-bound APTHS molecule with the aminopropyl group oriented parallel to the substrate (compare to Figure 4b). The PBE adsorption energies are essentially the same for both molecular orientations (see Table 1). If the D2* dispersion correction is included, the flat-lying species are slightly stabilized because of the proximity of the aminopropyl group to the surface, which suggests a preference of flat-lying molecules at low adsorbate coverage. However, the additional gain in adsorption energy is rather small (about 0.1−0.2 eV). In the presence of a solvent the additional interaction of the solvent molecules with the substrate can easily outweigh this small energy gain, so that an upright orientation of the linker molecules becomes also more favorable at low surface coverage.

The last binding mode considered in our study is the covalent cross-linking of hydrolyzed APTES molecules on the surface. Figure 5d shows two covalently bound APTHS which are coupled via an additional condensation reaction. Such coupling reactions may continue and a pair of linker molecules can be seen as a precursor for the formation of siloxane chains on the substrate. From the adsorption energies for single and cross-coupled linker units in Table 1 we can conclude that condensation reactions with the substrate are slightly more favorable than between APTHS molecules. Nevertheless, as we will show in the following, cross-linking will be an important structural motif in the APTHS layer on hydroxylated Mg substrates.

The adsorption energies in Table 1 suggest that physisorption is more favorable than covalent binding of the hydrolyzed APTES molecules to the substrate. However, in our definition of the adsorption energy we have assumed that the water molecules released in the condensation reactions are brought into vacuum at zero temperature. It is not taken into account that in experiment the water molecules will either attach to the surface or move into the solvent, thereby gaining cohesion energy and entropy. The free energy gain of water molecules released in the condensation reactions is given by the water chemical potential μ_W. Therefore, to be able to determine the thermodynamic stability of an adsorbate layer depending on the experimental conditions, the zero temperature gas phase value E^W_{mol} has to be replaced by the chemical potential μ_W as the reference energy of released water molecules.[41,58,59] E^W_{mol} is an upper limit for the water chemical potential.[60] By introducing $\Delta\mu_W = \mu_W - E^W_{mol}$ we take this upper limit as new zero-point of energy. By normalizing to the surface area A,

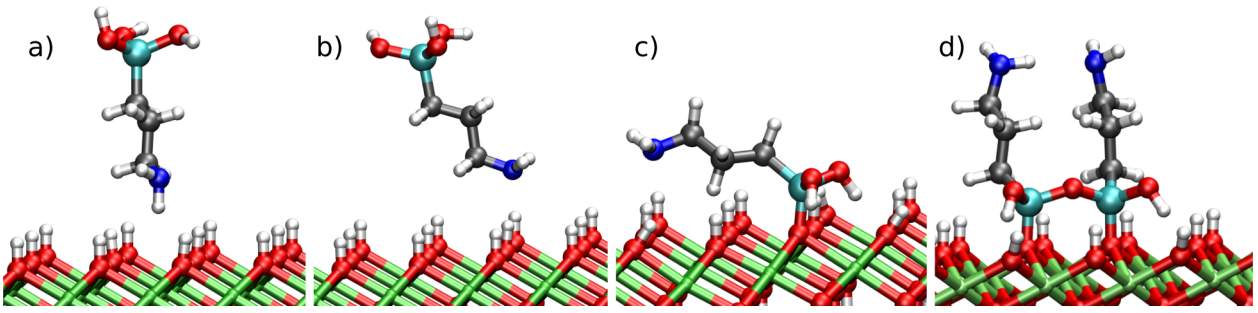

Figure 5. Alternative adsorption modes of hydrolyzed APTES on $Mg(OH)_2$: (a and b) via the amine functional group, (c) monodentate via the silanol group with additional interactions of the aminopropyl end with the substrate (compare to Figure 4b), and (d) with additional cross-coupling of two neighboring linker molecules. The same color coding as in Figure 4 is used.

DOI: 10.1021/am5075634
ACS Appl. Mater. Interfaces 2015, 7, 9006−9014

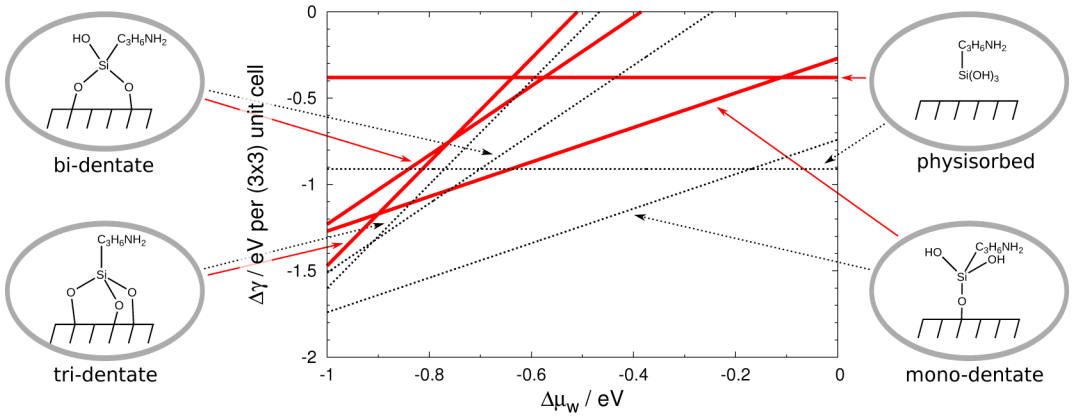

Figure 6. Surface phase diagram analyzing the relative stability of different binding modes of single hydrolyzed APTES molecules on $Mg(OH)_2$ as a function of the water chemical potential of the environment. Noncovalent and covalent binding after one, two and three condensation reactions with the substrate are shown. Solid red and dotted black lines refer to PBE and PBE+D2* results, respectively.

the adsorption energy of eq 1 is then converted to an interface energy between the surface and the environment as a function of the water chemical potential[58,59]

$$\Delta\gamma = [N\ E_{ad} + n\ \Delta\mu_W]/A \quad (3)$$

$\Delta\gamma$ is zero for the adsorbate-free surface. The most stable adsorbate structure at a given chemical potential can be identified as the one with the lowest interface energy.

The energies $\Delta\gamma$ for the four different binding modes of hydrolyzed APTES molecules via the $Si(OH)_3$ headgroup are shown in Figure 6. As expected, at high water chemical potential (approaching the zero temperature gas phase value), noncovalently bound, physisorbed species are energetically most stable. With lower water chemical potential, however, covalent binding becomes successively more favorable due to the free energy gain of the water molecules released in the condensation reactions (note that the slope of the graphs is given by the number of eliminated water molecules per linker unit).

To be able to identify the preferred binding mode under the conditions of the present experiments, a rough estimate for the corresponding water chemical potential is needed. $\Delta\mu_W$ of liquid water at ambient conditions is about −0.57 eV.[61,62] This is also roughly the interaction energy of water molecules with the $Mg(OH)_2$ substrate. If a residual water film on $Mg(OH)_2$ is the main reservoir with which molecules are exchanged in the condensation reactions, then the water chemical potential is close to −0.57 eV. Water molecules moving into the nominally water-free toluene solvent gain much less cohesive energy, which would correspond to a higher chemical potential. However, in the dilute state the water molecules have a high entropy and the chemical potential is lowered by $k_BT\ \ln(a_W)$, where a_W is the activity of water in toluene. Considering these uncertainties, −0.8 to −0.3 eV is a reasonable range for the water chemical potential reflecting the experimental conditions.

Figure 6 shows that in this range of $\Delta\mu_W$ not physisorption but chemisorption via a single condensation reaction in a monodentate geometry is the most favorable binding mode of APTHS molecules on hydroxylated Mg. This agrees very well with the experimental observation of Mg−O−Si fragments in the ToF-SIMS measurements and the high thermal stability of the SAMs upon heating. This conclusion is independent whether dispersion corrections are included in the calculations or not. Only at lower chemical potential (below −0.9 eV according to PBE results or below −1.1 eV if dispersion corrections are included) tridentate binding becomes thermodynamically more favorable, whereas bidentate binding is always higher in energy.

The thermodynamic analysis was also used to determine the stability of cross-coupled APTHS linker molecules on the hydroxylated Mg surfaces. The phase diagram in Figure 7

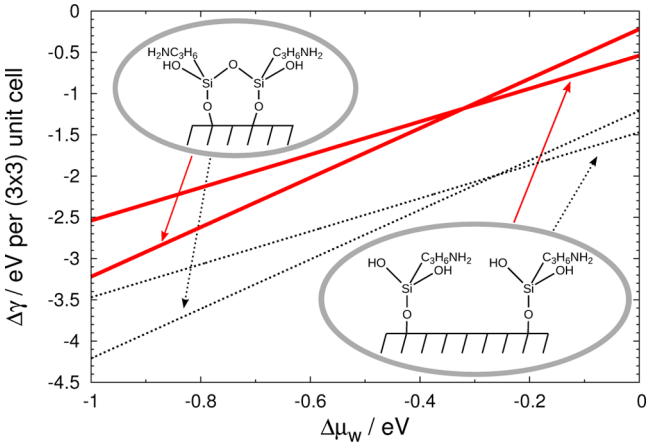

Figure 7. Surface phase diagram analyzing the competition between individual covalent binding of hydrolyzed APTES to the $Mg(OH)_2$ substrate by one condensation only and cross-coupling of the molecules by an additional condensation reaction. Solid red and dotted black lines refer to PBE and PBE+D2* results, respectively.

shows that for chemical potentials below −0.3 eV cross-coupling of neighboring molecules by additional condensation reactions becomes more favorable than having isolated linker molecules on the surface. Thus, at typical experimental conditions the thermodynamically most stable state are covalently bound linker molecules in a monodentate configuration, and a large fraction of the molecules will be cross-linked via elimination of another water molecule. Nevertheless, one has to keep in mind that kinetic limitations because of the activation barrier associated with the condensation reactions may also lead to a fraction of metastable configurations, for example, nonhydrolyzed APTES, or physisorbed and noncoupled molecules.

DOI: 10.1021/am5075634
ACS Appl. Mater. Interfaces 2015, 7, 9006−9014

CONCLUSIONS

In the present work, we investigated the interaction of the bifunctional molecule APTES, comprising an amino and an ethoxysilane functional group, with an hydroxylated Mg surface. XPS shows SAM formation of hydrolyzed APTES on the Mg substrate. The position of the N 1*s* signal indicates a free amine group, that is, coordination to the OH-terminated Mg substrate via the ethoxysilane groups. In ToF-SIMS, characteristic fragments of APTES strongly bound to the substrate occur as well as Mg−O−Si, reinforcing the assumption that APTES coordinates via a condensation reaction of the ethoxysilane moiety. Clear indication for physisorbed APTES could only be detected for multilayer coatings. The strong interaction of an APTES SAM with OH-terminated Mg is furthermore reinforced by the stability of the characteristic signals upon heating to 250 °C in UHV.

DFT calculations confirm the preference of the silanol over the amine group for the binding of hydrolyzed APTES molecules to the substrate. The calculations reveal that monodentate covalent attachment by elimination of one water molecule is more favorable than bi- and tridentate binding motives. The inclusion of van der Waals corrections significantly lowers the adsorption energies, but the relative stability of the structures is retained. A thermodynamic analysis shows that under the given experimental conditions the monodentate covalent binding is favored over physisorption of the linker molecules. In addition, the results strongly indicate that a large fraction of the covalently attached molecules is also cross-linked via a second condensation reaction.

ASSOCIATED CONTENT

Supporting Information

XPS data of the O 1s region, an assignment of all displayed ToF-SIMS signals, and the ToF-SIMS spectral regions showing the desorption of contaminants upon heating. This material is available free of charge via the Internet at http://pubs.acs.org.

AUTHOR INFORMATION

Corresponding Author

*Phone: +49 9131 8527575. E-mail: schmuki@ww.uni-erlangen.de.

Notes

The authors declare no competing financial interest.

ACKNOWLEDGMENTS

The authors thank Helga Hildebrand and Ulrike Marten-Jahns for XPS measurements. The work was supported by DFG via the Cluster of Excellence EXC 315 "Engineering of Advanced Materials" (EAM) and the Research Unit FOR 1878 "Functional Molecular Structures on Complex Oxide Surfaces" (funCOS). S.S. thanks the Fonds der Chemischen Industrie (FCI) for a Chemiefonds Fellowship.

REFERENCES

(1) Choi, S.-H.; Zhang Newby, B.-M. Suppress Polystyrene Thin Film Dewetting by Modifying Substrate Surface with Aminopropyltriethoxysilane. *Surf. Sci.* **2006**, *600*, 1391−1404.

(2) Costa, A. C.; Composto, R. J.; Vlcek, P.; Geoghegan, M. Block Copolymer Adsorption from a Homopolymer Melt to an Amine-Terminated Surface. *Eur. Phys. J. E: Soft Matter Biol. Phys.* **2005**, *18*, 159−166.

(3) Olmos, D.; Aznar, A. J.; Baselga, J.; Gonzalez-Benito, J. Kinetic Study of Epoxy Curing in the Glass Fiber/Epoxy Interface Using Dansyl Fluorescence. *J. Colloid Interface Sci.* **2003**, *267*, 117−126.

(4) Albala, R.; Olmos, D.; Aznar, A. J.; Baselga, J.; Gonzalez-Benito, J. Fluorescent Labels to Study Thermal Transitions in Epoxy/Silica Composites. *J. Colloid Interface Sci.* **2004**, *277*, 71−78.

(5) Watson, H.; Norstrom, A.; Torrkulla, A.; Rosenholm, J. Aqueous Amino Silane Modification of E-glass Surfaces. *J. Colloid Interface Sci.* **2001**, *238*, 136−146.

(6) Wang, B.; Huang, Y.; Liu, L. Effect of Solvents on Adsorption of Phenolic Resin onto γ-Aminopropyl-Triethoxysilane Treated Silica Fiber During Resin Transfer Molding. *J. Mater. Sci.* **2006**, *41*, 1243−1246.

(7) Enders, D.; Nagao, T.; Pucci, A.; Nakayama, T. Reversible Adsorption of Au Nanoparticles on SiO_2/Si: An In Situ ATR-IR Study. *Surf. Sci.* **2006**, *600*, 71−75.

(8) Kooij, E. S.; Brouwer, E. A. M.; Wormeester, H.; Poelsema, B. Ionic Strength Mediated Self-Organization of Gold Nanocrystals: An AFM Study. *Langmuir* **2002**, *18*, 7677−7682.

(9) Tang, H.; Zhang, W.; Geng, P.; Wang, Q.; Jin, L.; Wu, Z.; Lou, M. A New Amperometric Method for Rapid Detection of Escherichia Coli Density Using a Self-Assembled Monolayer-Based Bienzyme Biosensor. *Anal. Chim. Acta* **2006**, *562*, 190−196.

(10) Nakagawa, T.; Tanaka, T.; Niwa, D.; Osaka, T.; Takeyama, H.; Matsunaga, T. Fabrication of Amino Silane-Coated Microchip for DNA Extraction from Whole Blood. *J. Biotechnol.* **2005**, *116*, 105−111.

(11) Kim, J.-K.; Shin, D.-S.; Chung, W.-J.; Jang, K.-H.; Lee, K.-N.; Kim, Y.-K.; Lee, Y.-S. Effects of Polymer Grafting on a Glass Surface for Protein Chip Applications. *Colloids Surf., B* **2004**, *33*, 67−75.

(12) Killian, M. S.; Krebs, H. M.; Schmuki, P. Protein Denaturation Detected by Time-of-Flight Secondary Ion Mass Spectrometry. *Langmuir* **2011**, *27*, 7510−7515.

(13) Nanci, A.; Wuest, J. D.; Peru, L.; Brunet, P.; Sharma, V.; Zalzal, S.; McKee, M. D. Chemical Modification of Titanium Surfaces for Covalent Attachment of Biological Molecules. *J. Biomed. Mater. Res. B* **1998**, *40*, 324−335.

(14) Song, Y.-Y.; Schmidt-Stein, F.; Bauer, S.; Schmuki, P. Amphiphilic TiO_2 Nanotube Arrays: An Actively Controllable Drug Delivery System. *J. Am. Chem. Soc.* **2009**, *131*, 4230−4231.

(15) Killian, M. S.; Schmuki, P. Influence of Bioactive Linker Molecules on Protein Adsorption. *Surf. Interface Anal.* **2014**, *46*, 193−197.

(16) Killian, M. S.; Wagener, V.; Schmuki, P.; Virtanen, S. Functionalization of Metallic Magnesium with Protein Layers via Linker Molecules. *Langmuir* **2010**, *26*, 12044−12048.

(17) Wagener, V.; Killian, M. S.; Turhan, C. M.; Virtanen, S. Albumin Coating on Magnesium via Linker Molecules—Comparing Different Coating Mechanisms. *Colloids Surf., B* **2013**, *103*, 586−594.

(18) Witte, F.; Hort, N.; Vogt, C.; Cohen, S.; Kainer, K. U.; Willumeit, R.; Feyerabend, F. Degradable Biomaterials Based on Magnesium Corrosion. *Curr. Opin. Solid State Mater. Sci.* **2008**, *12*, 63−72.

(19) Witte, F.; Kaese, V.; Haferkamp, H.; Switzer, E.; Meyer-Lindenberg, A.; Wirth, C. J.; Windhagen, H. In Vivo Corrosion of Four Magnesium Alloys and the Associated Bone Response. *Biomaterials* **2005**, *26*, 3557−3563.

(20) Zeng, R.; Dietzel, W.; Witte, F.; Hort, N.; Blawert, C. Progress and Challenge for Magnesium Alloys as Biomaterials. *Adv. Eng. Mater.* **2008**, *10*, B3−B14.

(21) McBride, E. D. Absorbable Metal in Bone Surgery: A Further Report on the Use of Magnesium Alloys. *J. Am. Med. Assoc.* **1938**, *111*, 2464−2467.

(22) Witte, F.; Fischer, J.; Nellesen, J.; Crostack, H.-A.; Kaese, V.; Pisch, A.; Beckmann, F.; Windhagen, H. In Vitro and in Vivo Corrosion Measurements of Magnesium Alloys. *Biomaterials* **2006**, *27*, 1013−1018.

(23) Song, G. Control of Biodegradation of Biocompatible Magnesium Alloys. *Corros. Sci.* **2007**, *49*, 1696−1701.

DOI: 10.1021/am5075634
ACS Appl. Mater. Interfaces 2015, 7, 9006−9014

(24) Liu, C. L.; Xin, Y. C.; Tian, X. B.; Chu, P. K. Degradation Susceptibility of Surgical Magnesium Alloy in Artificial Biological Fluid Containing Albumin. *J. Mater. Res.* **2007**, *22*, 1806−1814.
(25) Rettig, R.; Virtanen, S. Time-Dependent Electrochemical Characterization of the Corrosion of a Magnesium Rare-Earth Alloy in Simulated Body Fluids. *J. Biomed. Mater. Res. A* **2008**, *85*, 167−175.
(26) Abel, E. W.; Pollard, F. H.; Uden, P. C.; Nickless, G. A New Gas-Liquid Chromatographic Phase. *J. Chromatogr. A* **1966**, *22*, 23−28.
(27) Roosmalen, A. J. v.; Mol, J. C. An Infrared Study of the Silica Gel Surface. 2. Hydration and Dehydration. *J. Phys. Chem.* **1979**, *83*, 2485−2488.
(28) Kallury, K. M. R.; Krull, U. J.; Thompson, M. X-Ray Photoelectron Epectroscopy of Silica Surfaces Treated with Polyfunctional Silanes. *Anal. Chem.* **1988**, *60*, 169−172.
(29) Wassermann, S. R.; Withesides, G. M.; Tidswell, I. M.; Ocko, B. M.; Pershan, P. S.; Axe, J. D. The Structure of Self-Assembled Monolayers of Alkylsiloxanes on Silicon: A Comparison of Results from Ellipsometry and Low-Angle X-ray Reflectivity. *J. Am. Chem. Soc.* **1989**, *111*, 5852−5861.
(30) Sagiv, J. Organized Monolayers by Adsorption. 1. Formation and Structure of Oleophobic Mixed Monolayers on Solid Surfaces. *J. Am. Chem. Soc.* **1980**, *102*, 92−98.
(31) Silverman, B. M.; Wieghaus, K. A.; Schwartz, J. Comparative Properties of Siloxane vs Phosphonate Monolayers on A Key Titanium Alloy. *Langmuir* **2005**, *21*, 225−228.
(32) Ohlhausen, J. A.; Zavadil, K. R. Time-of-Flight Secondary Ion Mass Spectrometry Measurements of a Fluorocarbon-Based Self-Assembled Monolayer on Si. *J. Vac. Sci. Technol. A* **2006**, *24*, 1172−1178.
(33) Helmy, R.; Fadeev, A. Y. Self-Assembled Monolayers Supported on TiO_2: Comparison of $C_{18}H_{37}SiX_3$ (X = H, Cl, OCH_3), $C_{18}H_{37}Si(CH_3)_2Cl$, and $C_{18}H_{37}PO(OH)$. *Langmuir* **2002**, *18*, 8924−8928.
(34) Horner, M. R.; Boerio, F. J.; Clearfield, H. M. An XPS Investigation of the Adsorption of Aminosilanes onto Metal Substrates. *J. Adhes. Sci. Technol.* **1992**, *6*, 1−22.
(35) Hook, D. J.; Vargo, T. G.; Gardella, J. A., Jr.; Litwiler, K. S.; Bright, F. V. Silanization of Radio Frequency Glow Discharge Modified Expanded Poly(Tetrafluoroethylene) Using (Aminopropyl)-triethoxysilane. *Langmuir* **1991**, *7*, 142−151.
(36) Nie, H.-Y. Revealing Different Bonding Modes of Self-Assembled Octadecylphosphonic Acid Monolayers on Oxides by Time-of-Flight Secondary Ion Mass Spectrometry: Silicon vs Aluminum. *Anal. Chem.* **2010**, *82*, 3371−3376.
(37) Killian, M. S.; Gnichwitz, J.-F.; Hirsch, A.; Schmuki, P.; Kunze, J. ToF-SIMS and XPS Studies of the Adsorption Characteristics of a Zn-Porphyrin on TiO_2. *Langmuir* **2010**, *26*, 3531−3538.
(38) Killian, M. S.; Wagener, V.; Schmuki, P. Adsorption Characteristics of a Zn-Porphyrin on MgO Surfaces. *Surf. Interface Anal.* **2013**, *45*, 194−197.
(39) Schmidt-Stein, F.; Hahn, R.; Gnichwitz, J. F.; Song, Y. Y.; Shresta, N. K.; Hirsch, A.; Schmuki, P. X-Ray Induced Photocatalysis on TiO_2 and TiO_2 Nanotubes: Degradation of Organics and Drug Release. *Electrochem. Commun.* **2009**, *11*, 2077−2080.
(40) Zorn, G.; Baio, J. E.; Weidner, T.; Migonney, V.; Castner, D. G. Characterization of Poly(Sodium Styrene Sulfonate) Thin Films Grafted from Functionalized Titanium Surfaces. *Langmuir* **2011**, *27*, 13104−13112.
(41) Bauer, T.; Schmaltz, T.; Lenz, T.; Halik, M.; Meyer, B.; Clark, T. Phosphonate- and Carboxylate-Based Self-Assembled Monolayers for Organic Devices: A Theoretical Study of Surface Binding on Aluminum Oxide with Experimental Support. *ACS Appl. Mater. Interfaces* **2013**, *5*, 6073−6080.
(42) Vaiss, V.; Berg, R.; Ferreira, A.; Borges, I.; Leitão, A. Theoretical Study of the Reaction Between HF Molecules and Hydroxyl Layers of $Mg(OH)_2$. *J. Phys. Chem. A* **2009**, *113*, 6494−6499.
(43) Vaiss, V.; Borges, I.; Leitão, A. Sarin Degradation Using Brucite. *J. Phys. Chem. C* **2011**, *115*, 24937−24944.
(44) Brzoska, J. B.; Ben Azouz, I.; Rondelez, F. Silanization of Solid Substrates: A Step Toward Reproducibility. *Langmuir* **1994**, *20*, 4367−4373.
(45) Song, Y.-Y.; Hildebrand, H.; Schmuki, P. Optimized Monolayer Grafting of 3-Aminopropyltriethoxysilane onto Amorphous, Anatase, and Rutile TiO_2. *Surf. Sci.* **2010**, *604*, 346−353.
(46) Kluth, G. J.; Sander, M.; Sung, M. M.; Maboudian, R. Study of the Desorption Mechanism of Alkylsiloxane Self-Assembled Monolayers through Isotopic Labeling and High Resolution Electron Energy-Loss Spectroscopy Experiments. *J. Vac. Sci. Technol.* **1998**, *16*, 932−936.
(47) Scofield, J. H. Hartree-Slater Subshell Photoionization Cross-Sections at 1254 and 1487 eV. *J. Electron Spectrosc. Relat. Phenom.* **1976**, *8*, 129−137.
(48) Reilmann, R. F.; Msezane, A.; Manson, S. T. Relative Intensities in Photoelectron Spectroscopy of Atoms and Molecules. *J. Electron Spectrosc. Relat. Phenom.* **1976**, *8*, 389−394.
(49) Giannozzi, P.; Baroni, S.; Bonini, N.; Calandra, M.; Car, R.; Cavazzoni, C.; Ceresoli, D.; Chiarotti, G. L.; Cococcioni, M.; Dabo, I.; Dal Corso, A.; de Gironcoli, S.; Fabris, S.; Fratesi, G.; Gebauer, R.; Gerstmann, U.; Gougoussis, C.; Kokalj, A.; Lazzeri, M.; Martin-Samos, L.; Marzari, N.; Mauri, F.; Mazzarello, R.; Paolini, S.; Pasquarello, A.; Paulatto, L.; Sbraccia, C.; Scandolo, S.; Sclauzero, G.; Seitsonen, A. P.; Smogunov, A.; Umari, P.; Wentzcovitch, R. M. QUANTUM ESPRESSO: A Modular and Open-Source Software Project for Quantum Simulations of Materials. *J. Phys.: Condens. Matter* **2009**, *21*, 395502.
(50) Vanderbilt, D. Soft Self-Consistent Pseudopotentials in a Generalized Eigenvalue Formalism. *Phys. Rev. B* **1990**, *41*, 7892−7895.
(51) Perdew, J. P.; Burke, K.; Ernzerhof, M. Generalized Gradient Approximation Made Simple. *Phys. Rev. Lett.* **1996**, *77*, 3865−3868.
(52) Grimme, S. Semiempirical GGA-Type Density Functional Constructed with a Long-Range Dispersion Correction. *J. Comput. Chem.* **2006**, *27*, 1787−1799.
(53) Tosoni, S.; Sauer, J. Accurate Quantum Chemical Energies for the Interaction of Hydrocarbons with Oxide Surfaces: CH_4/MgO-(001). *Phys. Chem. Chem. Phys.* **2010**, *12*, 14330−14340.
(54) Ehrlich, S.; Moellmann, J.; Reckien, W.; Bredow, T.; Grimme, S. System-Dependent Dispersion Coefficients for the DFT-D3 Treatment of Adsorption Process on Ionic Surfaces. *Chem. Phys. Chem.* **2011**, *12*, 3414−3420.
(55) Seiler, S.; Meyer, B. in preparation.
(56) Catti, M.; Ferraris, G.; Hull, S.; Pavese, A. Static Compression and H Disorder in Brucite, $Mg(OH)_2$, to 11 GPa: A Powder Neutron Diffraction Study. *Phys. Chem. Miner.* **1995**, *22*, 200−206.
(57) Kosmulski, M. Compilation of PZC and IEP of Sparingly Soluble Metal Oxides and Hydroxides from Literature. *Adv. Colloid Interface Sci.* **2009**, *152*, 14.
(58) Meyer, B. First-Principles Study of the Polar O-Terminated ZnO Surface in Thermodynamic Equilibrium with Oxygen and Hydrogen. *Phys. Rev. B* **2004**, *69*, 045416.
(59) Meyer, B.; Rabaa, H.; Marx, D. Water Adsorption on $ZnO(10\bar{1}0)$: From Single Molecules to Partially Dissociated Monolayers. *Phys. Chem. Chem. Phys.* **2006**, *8*, 1513−1520.
(60) Qian, G.-X.; Martin, R. M.; Chadi, D. J. First-Principles Study of the Atomic Reconstructions and Energies of Ga- and As-Stabilized GaAs(100) Surfaces. *Phys. Rev. B* **1988**, *38*, 7649−7663.
(61) Klaumünzer, M.; Mačković, M.; Ferstl, P.; Voigt, M.; Spiecker, E.; Meyer, B.; Peukert, P. Phase Transition Behavior and Oriented Aggregation During Precipitation of $In(OH)_3$ and InOOH Nanocrystals. *J. Phys. Chem. C* **2012**, *116*, 24529−24537.
(62) Weast, R. C., Ed. *Handbook of Chemistry and Physics*, 65th ed.; CRC Press: Boca Raton, FL, 1984.

DOI: 10.1021/am5075634
ACS Appl. Mater. Interfaces 2015, 7, 9006−9014